Molecular Docking Studies on Gingerol Analogues toward Mushroom Tyrosinase

[1]Sabrina. Benouis*, [1]Fouad. Ferkous, [1,2]Khairedine. Kraim, [3]Ahmed. Allali, [1]Youcef. Saihi
[1]Laboratoire de chimie organique appliquée, Faculté des Sciences, Université BADJI Mokhtar, BP12, 23000 Annaba, Algérie.
[2]Ecole normale supérieure d'enseignement technologique de Skikda(ENSET), 21000, Azzaba Skikda.
[3]Département des Sciences Biologiques, Université d'El Oued, BP 789, 39000, El Oued-Algérie.
ferkousf@yahoo.fr: youcefchem@gmail.com*

(Received on 11th May 2018, accepted in revised form 12th July 2019)

Summary: The gingerol presents the starting point of our work which aims to discover new inhibitors of the tyrosinase enzyme. Therefore, we have studied the activity of gingerol derivatives as inhibitors against mushroom tyrosinase based on the molecular docking.
Molecular docking studies were performed on a series of gingerol analogues retrieved from Zinc database (with 70% as similarity threshold). The gingerol analogues were docked within the active site region of mushroom tyrosinase (PDB: 2Y9X) using Molegro Virtual Docker V.5.0.
The results of molecular docking studies revealed that some analogues of gingerol have higher Moldock score (in terms of negative energy) than gingerol and the experimentally known inhibitors of tyrosinase, and showed favourable molecular interactions exhibiting common molecular interaction with Ala323, Met280 and Asn260 residues of tyrosinase. Furthermore, the top docked compounds used in this work do not violate the Lipinsky rule of five.

Keywords: Gingerol, Molecular docking, Tyrosinase, Inhibition, Molegro Virtual Docker.

Introduction

Since antiquity, nature has been a source of the majority of medicines, cosmetics and bioactive compounds [1, 2]. Until now, plants play a vital role in the pharmacological, agricultural and food industry [3]. Among these famous plants ginger scientifically known as (*Zingiber officinale roscoe*) that is largely used for food spicing [4], this plant is endowed with antioxidant [5,6], inflammatory [7], antimicrobial [8], anticoagulant [9] and others pharmacological activities proven in the literature [10,11].

The medicinal benefits of ginger are mainly due to the presence of gingerol which is one of the bioactive molecules recognized for these pharmacological activities [12, 13] such as anti-oxidant [14], anti-inflammatory [15], and anti-cancer properties [16]. Moreover, an inhibition of melanogenesis was reported in vitro by gingerol as an effective depigment agent [17, 18]. Tyrosinase is the enzyme responsible for the production of melanin [19], natural substance responsible for the pigmentation of the skin [20]. The Gingerol presents the starting point of our work which aims to discover new inhibitors of the enzyme tyrosinase. In this study, we have realized a virtual screening based on molecular docking of 1280 analogues of gingerol as inhibitors against the mushroom tyrosinase. The aim of this work is to identify the binding mode of the active molecules and to predict the affinity of ligand and protein using Moldock scoring function installed in the MVD program.

Experimental

Target Enzyme

The Tyrosinase, from *Agaricus bisporus* mushroom, was selected as the target enzyme. The three dimensional structure of the target enzyme was taken from the Protein Data Bank (PDB ID: 2Y9X) [21]. The selected target (ID: 2Y9X) represents the L4H4 octamer (four L-H dimer) crystal structures of tyrosinase from Agaricus Bisporus mushroom [22] with a resolution of 2.78 Å. The tyrosinase domain represented by the H1 subunit and containing the binuclear copper binding site is selected to perform the molecular docking studies [23]. The active site complexed with the reference inhibitor tropolone is conserved with the binuclear copper atoms. The water molecules are removed from the binding site and the enzyme was prepared with Molegro Virtual Docker by adding hydrogen atoms, and all atoms types and bond orders were corrected.

Ligands dataset: chemical similarity searching

The three-dimensional structure of gingerol (ZINC1531846) and those of its analogues were retrieved from the public free ZINC database [24]. We have adopted the tanimito coefficient as search parameters with 70% as similarity threshold. All obtained structures are saved as "mol2" files for our docking studies. The library is prepared then with MVD program.

Molecular docking

The binding affinity between ligand and enzyme, when the three dimensional structure is known, is treated with molecular docking. Here the molecular docking studies were performed with the program

***To whom all correspondence should be addressed.**

Molegro Virtual Docker. The program is based on three principal algorithms: Moldock scoring function, conformational search algorithm and cavity prediction algorithm, represented as follow:

*MolDock Scoring Function***:** proposed by Gelhaar et al. [25] and is composed of two terms representing respectively the intramolecular energy (the interaction between atoms of the same ligand) and external interaction energy (ligand–protein). The pose energy (enzyme–ligand) is represented by the sum of these two energy terms and their expressions are defined as follow:

$$E_{score} = E_{inter} + E_{intra}$$

where:

E_{inter} and E_{intra} are the ligand–protein energy interaction and the ligand internal energy respectively.

$$E_{inter} = \sum_{i \in ligand} \sum_{j \in protein} \left[E_{PLP}(r_{ij}) + 332.0 \frac{q_i q_j}{4r_{ij}^2} \right]$$

where:

- E_{PLP} : is piecewise linear potential function;
- q_i and q_j: are the electrical charges of the atoms *i* and *j*;
- r_{ij}: is the distance between the two aotms *i*and *j* (*i* is ligand atom, and *j* is protein atom).

$$E_{intra} = \sum_{i \in ligand} \sum_{j \in ligand} E_{PLP}(r_{ij}) + \sum_{flexiblebonds} [1 - \cos(n\phi - \phi_0)] + E_{clash}$$

where:

- The first term calculates all the energies involving pairs of atoms of the ligand, except those connected by two bonds;
- The last two terms represent respectively the torsional energy and a penalty of 1000 kcal/mol if the distance between two heavy atoms is less than 2.0Å.

MolDock Optimizer

Moldock Optimizer, used as a search algorithm by the MVD program, is an iterative optimization technique inspired from the evolution theory of Darwin. The Moldock algorithm randomly generates the first population. Then, the poor solutions are weeded out and the good candidate solutions are selected and modified using crossover and mutation operations between the candidate solutions (poses) [25].

Cavity prediction

The program Molegro Virtual Docker uses grid–based prediction algorithm in order to determine the binding site. This algorithm divides the protein space into a discrete grid with a resolution of 0.8Å and at each point of the grid is placed a sphere of radius 1.4Å. The detected cavities are ranked according to their volume.

The binding site was detected, selected as search space and centred on the co-crystallized troplone with a radius of 14Å. During the docking simulation, the program generates several poses for each ligand using the Moldock scoring function and Moldock optimizer algorithms. The parameters of the last algorithm: the population size, maximum iterations, scaling factor, and crossover rate were set to 100; 9000; 0.50 and 0.90 respectively. For each complex, the molecular docking simulation was executed 100 runs while each run returns one pose. The resulting poses were visualized in Table 1.

Table-1: Docking score for the top ten ranked hits and known experimentally tyrosinase inhibitors.

Compound ID	E-Inter (cof - lig)[a] (kcal.mol^{-1})	E-Inter (pro - lig)[b] (kcal.mol^{-1})	E-Inter total[c] (kcal.mol^{-1})	MolDock score (kcal.mol^{-1})	H-bond energy[d] (kcal.mol^{-1})
ZINC13377891	**-3.93**	**-164.30**	**-168.23**	**-157.15**	**-8.12**
ZINC13377888	**-4.81**	**-162.68**	**-167.49**	**-155.86**	**-4.55**
ZINC31169866	**-5.14**	**-157.80**	**-162.94**	**-150.75**	**-15.09**
ZINC13377906	**-5.077**	**-158.57**	**-163.65**	**-149.68**	**-16.16**
ZINC04649679	**-2.47**	**-153.36**	**-155.83**	**-142.06**	**-7.87**
ZINC31169874	**-4.38**	**-149.35**	**-153.73**	**-141.75**	**-10.62**
ZINC13130926	**-4.79**	**-146.99**	**-151.78**	**-139.13**	**-6.20**
ZINC01681526	**-3.39**	**-142.74**	**-146.13**	**-137.53**	**-3.06**
ZINC15112765	**-4.42**	**-155.01**	**-159.43**	**-137.49**	**-6.80**
ZINC31159224	**-4.37**	**-150.55**	**-154.93**	**-135.97**	**-11.83**
Gingerol	**-4.18**	**-130.67**	**-134.85**	**-130.67**	**-1.43**
Kojic acid	**-1.85**	**-81.91**	**-81.76**	**-81.26**	**-4.63**
Hydroquinone	**-3.09**	**-63.70**	**-65.87**	**-58.25**	**-4.28**
tropolone	**-2.18**	**-75.94**	**-79.04**	**-77.09**	**-3.11**

[a]: The total ligand-cofactor interaction energy.
[b]: The total pose-protein interaction energy.
[c]: The total interaction energy.
[d]: Hydrogen bonding energy.

Results and Discussions

The protein structure complex of the inhibitor of reference with tyrosinase enzyme (PDB ID: 2Y9X) was obtained from the Protein database. The potential ligand binding cavity was predicted using Molegro Virtual Docker for the mushroom tyrosinase which has a volume of 50.69Å^3 and a surface area of 197.12Å^2 (Fig 1).

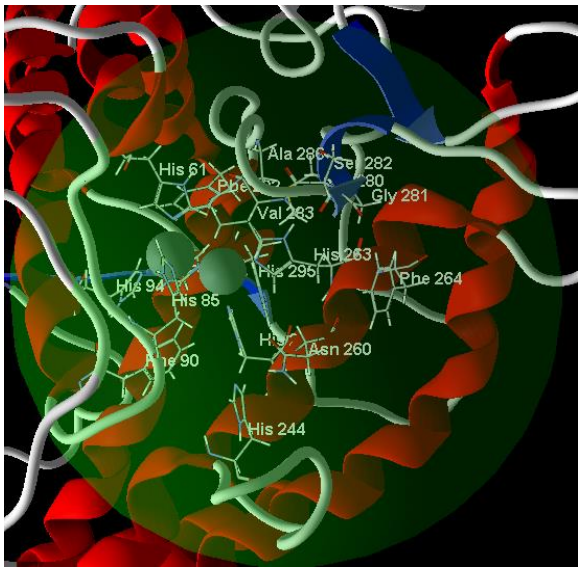

Fig. 1: The binding cavity of tyrosinase enzyme with residues Phe264, Phe90, His94, His244, Phe292, Ala286, Val283, Gly281, Met280, Asn260, Ser282, His85, His61, His263, His259, His296 and copper ions represented by two silver balls.

Molecular docking was carried out and the top poses docked at the active site region of tyrosinase were ranked according to the MolDock score energy (Table 1). According to th obtained docking result, we notice that the gingerol analogues (zinc13377891, zinc13377888, zinc31169866, zinc13377906, zinc04649679, zinc31169874, zinc13130926, zinc01681526, zinc15112765, zinc31159224) have higher MolDock scores (in term of negative energy) than gingerol and the experimentally known tyrosinase inhibitors.

The top ranked gingerol analogues present a high level of ligand-protein interaction energy compared to gingerol and experimentally tyrosinase inhibitors like Kojic acid [26], hydroquinone [27] and tropolone [28]. The correlation between the hydrogen bonding energy and molecular weight for the top ranked compounds is calculated and depicted in Fig 2. A low value of determination coefficient (0.049) was obtained, which indicates that the predicted hydrogen bonding energy was mainly because of structure features and not because of its molecular size.

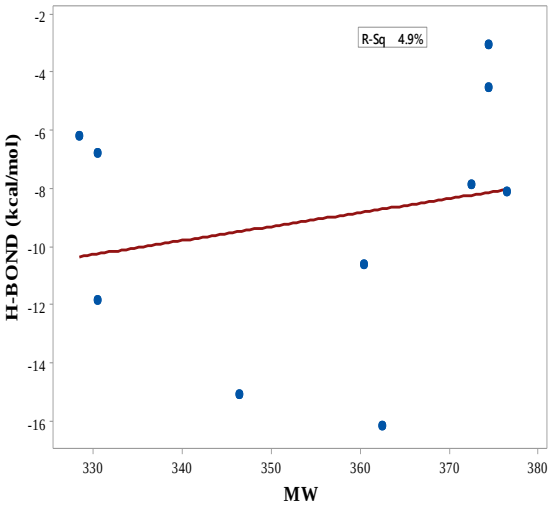

Fig. 2: Fitted line plot of the correlation between interaction energy and molecular weight.

In order to have a deep structural insight for the interaction between the selected top ten compounds and our target, further analysis based on both electrostatic and hydrogen bonds is carried out (Table-2).

Table-2 lists all the major predicted interactions between the top ten hits and the tyrosinase active site residues, exhibiting the interaction energy ligand-protein, the present residues and the interaction distances. The binding modes of the top hits reveal that these latter were found to be docked into the binding site of tyrosinase (Fig 3).

According to the different binding modes of the top ten hits, it is observed that the interactions with the amino acids Met28 and Asn260 of the tyrosinase active site are the most predominant among the top hits. It is also observed that the top two hits Zinc13377891 and Zinc13377888 have a common ineraction with the Met280, Ala323 and Asn260 residues of tyrosinase.

Table-2: Ligand structure, present residues, ligand-protein interaction energy and interaction distances for the top hits.

Compound ID	Structure	Residue	Interaction distance (Å)	Interaction energy (kcal.mol^{-1})
Zinc13377891	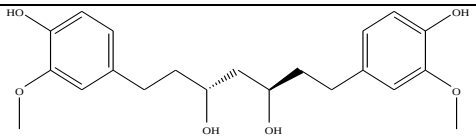	Ala323	2.86	-0.64
		Asn260	2.95	-1.46
		His240	3.39	-1.03
		His240	2.74	-2.50
		Met280	2.99	-2.50
Zinc13377888	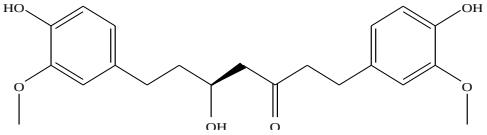	Ala323	3.05	-2.50
		Asn260	2.96	-1.17
		Asn260	3.40	-0.99
		His85	3.49	-0.54
		Met280	2.60	-2.50
		Ser282	3.57	-0.02
Zinc31169866	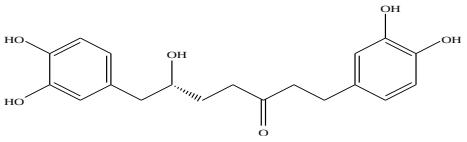	Glu322	3.01	-2.30
		Glu322	3.11	-2.19
		Glu322	3.23	-1.48
		Thr84	3.53	-0.11
		Asn320	2.60	-0.59
		Val283	3.20	-2.00
		Met280	2.77	-2.50
Zinc13377906	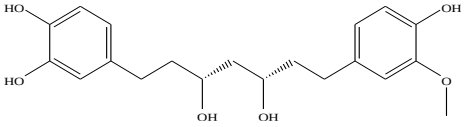	Asn260	3.20	-1.42
		Glu256	3.09	-2.50
		Val283	3.20	-1.99
		Met280	2.72	-2.50
		Asn260	2.89	-1.82
		His244	3.00	-2.46
		His244	2.86	-2.50
		Cys83	2.60	-2.38
		His85	3.04	-2.50
Zinc04649679	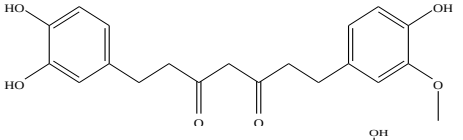	Asn260	2.87	-0.37
		Cys83	2.75	-2.50
		His85	3.05	-2.50
		Met280	2.99	-2.50
Zinc31169874	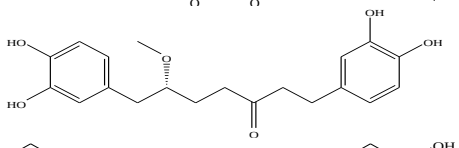	Asn260	2.98	-0.83
		Val283	3.56	-0.19
		Asn81	3.06	-2.50
		Cys83	2.60	-2.50
		Cys83	3.33	-1.37
		Met280	2.76	-2.08
Zinc13130926	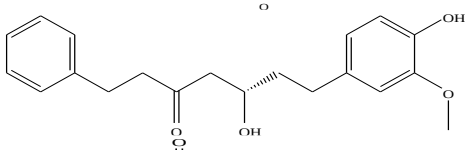	Asn260	3.07	-1.18
		Asn260	2.77	-2.50
		Met280	2.60	-2.50
		Ser282	3.55	-0.02
Zinc01681526	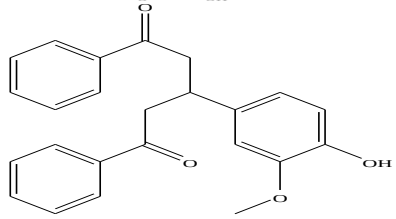	Asn260	2.91	-0.93
		Ser282	3.41	-0.93
		Val283	2.92	-2.13
Zinc15112765	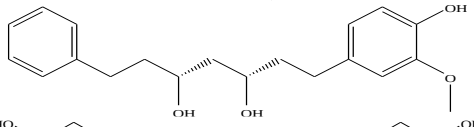	His244	3.10	-2.50
		Asn260	3.10	-1.79
		Met280	2.60	-2.46
		Glu256	2.99	-0.04
		Ser282	3.52	-0.02
Zinc31159224	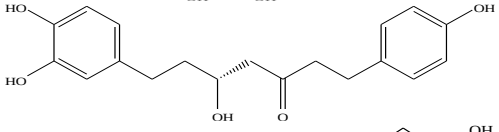	Gly245	3.05	-2.50
		Asn260	3.01	-1.85
		His244	2.98	-2.50
		Met280	3.09	-2.50
		Met280	2.60	-2.47
Gingerol	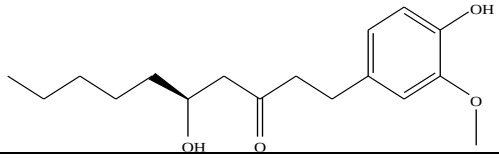	Met280	3.28	-1.59

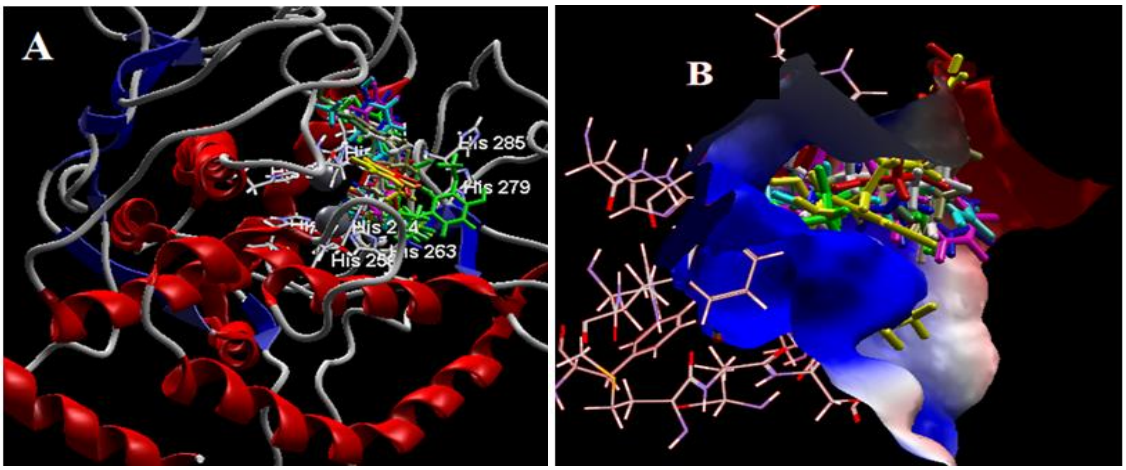

Fig. 3: (a) Top ten hits docked into the active site of tyrosinase and b) electrostatic surface view of tyrosinase showing the top ten docking hits inside the binding site.

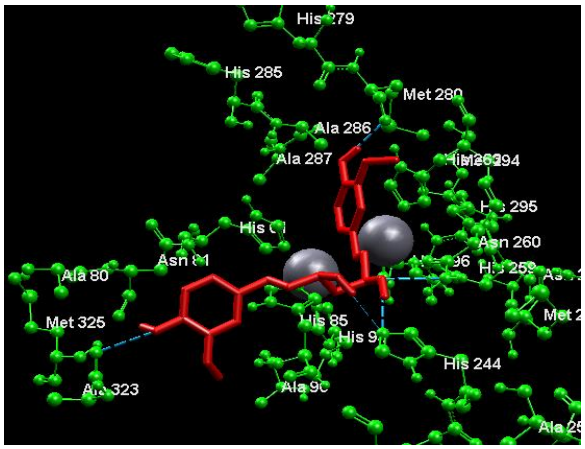

Fig. 4: Predicted H-bond interactions (blow dashed lines) linking ZINC13377891 (red) with Ala323, His244, Asn260, Met280 residues of tyrosinase enzyme.

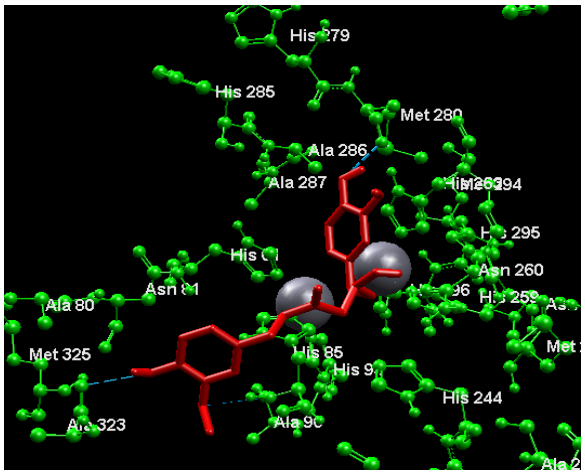

Fig. 5: Predicted H-bond interactions (blow dashed lines) between ZINC13377888 (red) and Ala323, His85, Asn260, Met280 residues of tyrosinase enzyme.

The top-scored pose Zinc13377891 forms five hydrogen bonds with four amino acid residues (Fig 4). The oxygen atom (ID 28) of hydroxyl group mediated a hydrogen bond with N atom (ID 2129) of Asn260 at distance of 2.59Å. The same atom of top-scored pose is also involved in a hydrogen bonding interaction with nitrogen atom (ID 2018) of His244 at distance of 2.74Å. The oxygen atom (ID 27) of hydroxyl group formed a hydrogen bond with the nitrogen atom (ID 2018) of His244 at distance of 3.39Å. Finally, two hydrogen bonds were formed between the oxygen atoms (ID 8 and ID 26) oxygen atoms of carbonyl groups (ID 2635 and ID 2228) of Ala323 and Met280 respectively. The positions in the active site of tyrosinase and the binding modes of the top two compounds (ZINC13377891 and ZINC13377888) and gingerol are shown in Fig 4, Fig 5 and Fig 6 respectively. The comparison between binding modes of these compounds reveals that the binding affinity of ZINC13377891 and ZINC13377888 with the active site residues of tyrosinase is more favorable than that of gingerol.

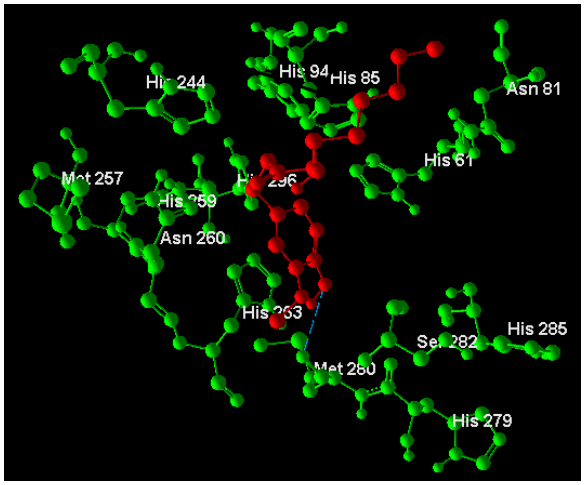

Fig. 6: Predicted H-bond interactions (blow dashed lines) between gingerol (red) and Met280 residue of tyrosinase enzyme.

The rule of five, described by Lipinski et al [29,30], states that most drug-like molecules have values of LogP (the logarithm of octanol/water partition coefficient) < 5, MW (molecular weight) < 500, HBA (number of hydrogen bond acceptors) < 10 and HBD (number of hydrogen bond donors) < 5. Molecules do not respect these rules may have problem with bioavailability [31].

Table3 represents the parameters values of the rule of five for the top ranked hits, gingerol and the experimentally known tyrosinase inhibitors. According to the values showed in table 3, all the top ranked hits used in this work abide by the Lipinski rule and may be active compounds.

Table-3: Parameters values of the Lipinski rule for the top hits and gingerol.

Compound ID	LogP[a]	MW[b]	HBA[c]	HBD[d]	TPSA[e]	ROT-B[f]
ZINC13377891	2.05	376.443	6	4	99.38	10
ZINC13377888	1.97	374.428	6	3	96.22	10
ZINC31169866	1.52	346.374	6	5	118.22	8
ZINC13377906	1.83	362.417	6	5	110.38	9
ZINC04649679	4.16	372.412	4	2	66.76	10
ZINC31169874	1.89	360.401	6	2	93.06	9
ZINC13130926	1.75	328.402	6	4	107.22	9
ZINC01681526	2.77	374.429	4	2	66.76	8
ZINC15112765	2.85	330.418	4	3	69.92	9
ZINC31159224	3.21	330.375	4	1	55.76	8
gingerol	3.23	294.386	4	2	66.00	10

[a]: The logarithm of octanol/water partition coefficient.
[b]: The molecular weight.
[c]: The number of hydrogen bond acceptors.
[d]: The number of hydrogen bond donors.
[e]: The topological polar surface area.
[f]: The number of rotatable bonds.

Conclusion

In this work, molecular docking studies were performed on gingerol analogues retrieved from the ZINC database. The results obtained from docking indicate that some analogues showed a higher Moldock score (in terms of negative energy) compared to gingerol and the experimentally known tyrosinase inhibitors. The top ten ranked hits showed better interaction than gingerol, showing a common molecular interaction with the Met280 and Asn260 residues of the tyrosinase enzyme. Furthermore, these ten docked hits abide by Lipinski's rule of five, stating that these molecules have no problem with bioavailability. In perspective, the best ranked molecular docking compounds will be tested experimentally and optimized in order to enrich the therapeutic class of tyrosinase inhibitors

Acknowledgments:

This study was supported by "la direction générale de la recherche scientifique et de développement thechnologique (DGRSDT)" of Algerian Ministry of Scientific Research. The authors dedicated this work to the memory of their colleague Dr.AZZOUZI Abdelkader.

References

1. G. Cragg and D. Newman, Natural Products: A Continuing Source Of Novel Drug Leads, *Biochim. Biophys. Acta*., **1830**, 3670 (2013).
2. S. Shakya, Medicinal Uses Of Ginger (*Zingiber officinale roscoe*) Improves Growth And

Enhances Immunity In Aquaculture, *Int. J. Chem .Stud*., **3**, 83 (2015).
3. A. Atanasov, B. Waltenberger, E. Pferschy-Wenzig, T. Linder, C. Wawrosch, P. Uhrin, V. Temml, L. Wang, S. Schwaiger, EH. Heiss, JM. Rollinger, D. Schuster, JM. Breuss, V. Bochkov, MD. Mihovilovic, B. Kopp, R. Bauer, V. M. Dirsch and H. Stuppner, Discovery And Resupply Of Pharmacologically Active Plant-Derived Natural Products, *Biotechnol. Adv*., **33**, 1582 (2015).
4. K. Srinivasan, Ginger Rhizomes (*Zingiber officinale*): A Spice With Multiple Health Beneficial Potentials, *Pharma. Nutrition.*, **5**, 18 (2017).
5. K. Danwilai, J. Konmun, B. Sripanidkulchai and S. Subongkot, Antioxidant Activity Of Ginger Extract As Daily Supplement In Cancer Patients Receiving Adjuvant Chemotherapy: A Pilot Study, *Cancer. Manag. Res*., **9**, 11 (2017).
6. W. Wenhui, Y. Chen, J. Zhang, Z. Chen and H. Chung, Antioxidant Activities of Ginger Extract And Its Constituents Toward Lipids, *Food. Chem*., **239**, 1117 (2018).
7. P. Wilson, Ginger (*Zingiber officinale*) As an Analgesic and Ergogenic Aid in Sport: A Systemic Review, *J. Strength. Cond. Res*., **29**, 2980 (2015).
8. A. Murugesan and B. Sivapathasundharam, Inhibitory Effects Of Ginger Extract On Candida Albicans, Staphylococcus Aureus And Lactobacillus Acidophilus, *Int. dent. med j. adv res*., **2**, 1 (2016).
9. O. Ajala, S. Ogunmade, T. Adelkan and K. Oyewole, Anticoagulant Activity Of Ginger (*Zingiber officinale roscoe, Zingiber aceae*) Rizhome Extract, *Nig. J. Pharm. Res*., **13**, 167 (2017).
10. J. Dhanik, N. Arya and V. Nand, A Review On *Zingiber officinale*, *J. Pharmacogn. Phytochem*., **6**, 174 (2017).
11. R. Wakchaure and S. Ganguly, In *Molecular Biology and Pharmacognosy and Beneficial Plants, Phytochemistry and pharmacological properties of ginger (Zingiber officinale)*, Editor. Lenin. Media. Pvt. LTD, Delhi, India, p. 97 (2018).
12. S. Wang, C. Zhang, G. Yang and Y. Yang, Biological Properties Of 6-Gingerol: A Brief Review, *Natural. Product. Communications*., **9**, 1027 (2014).
13. B. O. Ajayi, I. A. Adedara and E. O. Farombi, Pharmacological Activity Of 6-Gingerol In Dextran Sulphate Sodium-Induced Ulcerative Colitis In BALB/C Mice, *Phytother. Res*., **29**, 566 (2015).
14. H. Mi, X. Guo and J. Li, Effect Of 6-Gingerol As Natural Antioxidant On The Lipid Oxidation In Red Drum Fillets During Refrigerated Storage LWT, *J. Food Sci. Technol*., **74**, 70 (2016).
15. J. L. Funk, J. B. Frye, J. N. Oyarzo, J. Chen, H. Zhang and B. N. Timmermann, Anti-Inflammatory Effects Of The Essential Oils Of Ginger (*Zingiber Officinale Roscoe*) In Experimental Rheumatoid Arthritis, *Pharma. Nutrition.*, **4**, 123 (2016).
16. F. Zhang, K. Thakur, F. Hu, J. G. Zhang and Z. J. Wei, Cross-Talk Between 10-Gingerol And Its Anti-Cancerous Potential, *Food. Funct*., **8**, 2635 (2017).
17. H. C. Huang, S. H. Chiu and T. M. Chang, Inhibitory Effect Of [6]-Gingerol On Melanogenesis In B16f10 Melanoma Cells And A Possible Mechanism Of Action, *Biosci. Biotechnol. Biochem.*, **75**, 1067 (2011).
18. L. Zhang, G. Tao, J. Chen and Z. P. Zheng, Characterization Of A New Flavone And Tyrosinase Inhibition Constituents From The Twigs Of Morus Alba L, *Molecules*., **21**, 1130 (2016).
19. F. Yu, Z. Pan, B. Qu, X. Yu, K. Xu, Y. Deng and F. Liang, Identification Of A Tyrosinase Gene And Its Functional Analysis In Melanin Synthesis Of Pteria Penguin, *Gene*., **656**, 1 (2018).
20. K. U. Zaidi, S. A. Ali and A. S. Ali, Melanogenic Effect of Purified Mushroom Tyrosinase On B16f10 Melanocytes: A Phase Contrast And Immunofluorescence Microscopic Study, *J. Microsc. Ultrastruct*., **5**, 82 (2017).
21. www.rcsb.org
22. W. T. Ismaya, H. J. Rozeboom, A. Weijn, J. J. Mes, F. Fusetti, H. J. Wichers and B. W. Dijkstra, Crystal Structure Of Agaricus Bisporus Mushroom Tyrosinase: Identity Of The Tetramer Subunits And Interaction With Tropolone, *Biochemistry*., **50**, 5477 (2011).
23. W. T. Ismayaa, O. M. Tandrasasmitaa, S. Sundaria, A. Diana, X. Lai, D. S. Rentnoningrum, B.W. Dijkstra, R. R. Tjandrawinata and H. Rachmawati, The Light Subunit Of Mushroom *Agaricus Bisporus* Tyrosinase: Its Biological Characteristics And Implications, *Int. J. Biol. Macromol*., **102**, 308 (2017).
24. zinc15.docking.org
25. R. Thomsen and M. Christensen, Moldock: A New Technique For High-Accuracy Molecular Docking, *J. Med. Chem*., **49**, 3315 (2006).
26. B. K. Singh, S. H. Park, H. B. Lee, Y. H. Goo, H. S. Kim, S. H. Cho, J. H. Lee, G. W. Ahn, J. P. Kim, S. M. Kang and E. K. Kim, Kojic Acid

Peptide: A New Compound With Anti-Tyrosinase Potential, *Ann. Dermatol*., **28**, 555 (2016).
27. T. Pillaiyar, M. Manickam and V. Namasivayam, Skin Whitening Agents: Medicinal Chemistry Perspective Of Tyrosinase Inhibitors, *J. Enzyme. Inhib. Med. Chem*., **32**, 403 (2017).
28. R. Nairn, W. Cresswell and J. Nairn, Mushroom Tyrosinase: A Model System To Combine Experimental Investigation Of Enzyme-Catalyzed Reactions, Data Handling Using R, And Enzyme-Inhibitor Structural Studies, *Biochem. Mol. Biol. Educ*., **43**, 370 (2015).
29. C. A. Lipinski, Drug-Like Properties And The Causes Of Poor Solubility And Poor Permeability, *J. Pharmacol. Toxicol. Methods*., **44**, 235 (2000).
30. C. A. Lipinski, F. Lombardo, B. W. Dominy and P. J. Feeney, Experimental And Computational Approaches To Estimate Solubility And Permeability In Drug Discovery And Development Settings, *Adv. Drug. Del. Rev*., **23**, 3 (1997).
31. M. P. Freitas, MIA-QSAR Modelling Of Anti-HIV-1 Activities Of Some 2-Amino-6-Rylsulfonyl Benzonitriles And Their Thio And Sulfinyl Congeners. *Org. Biomol. Chem.*, **4**, 1154 (2006).